

1
2
3 Formation of intracellular glutamine synthetase bodies depends strongly upon cellular age and
4 glucose availability

5
6 **Jeremy O'Connell^{1*}, Mark Tsechansky^{1,2*}, Marguerite West-Driga¹, Edward M.
7 Marcotte^{1,‡}**

8
9 ¹Center for Systems and Synthetic Biology, Department of Molecular Biosciences, Institute for
10 Cellular and Molecular Biology, University of Texas at Austin, Austin, Texas, USA

11
12 ²Department of Chemistry, Cambridge University, Lensfield Road, Cambridge, UK

13
14 *These authors contributed equally to this work

15
16 *Running title: Glutamine synthetase body formation varies with cellular age and glycolytic flux

17
18 ‡ To whom correspondence should be addressed: Edward M. Marcotte, Center for Systems and
19 Synthetic Biology, Department of Molecular Biosciences, Institute for Cellular and Molecular
20 Biology, University of Texas at Austin, Austin, Texas, USA, MBB 3.148BA. Phone: (512)471-
21 5435, Fax: (512)232-3472, E-mail: marcotte@icmb.utexas.edu.
22

23 **ABSTRACT**

24 The enzyme glutamine synthetase serves key roles in central nitrogen metabolism, catalyzing the
25 biosynthesis of glutamine, as well as regulating ammonia assimilation and integrating metabolic
26 signals to balance nitrogen use. The budding yeast enzyme was recently found to form
27 intracellular bodies (GS bodies) composed of glutamine synthetase and Hsp90 chaperones
28 following various types of nutrient depletion or chemical stress. In order to better quantify and
29 characterize the *in vivo* formation of GS bodies, we developed an assay for their formation in
30 single yeast cells using imaging flow cytometry, which enables the quantitative measurement of
31 rates of GS body formation and their population penetrance. Either reduction of supplied
32 glucose, or addition of the competitive inhibitor of glycolysis, 2- deoxyglucose, markedly
33 enhanced the formation of GS bodies. The occurrence of GS bodies increased with increasing
34 cell size, a proxy for cell age, while treatment with rapamycin antagonized their formation.
35 Direct measurement of GS body formation as a function of replicative age showed that mother
36 cells exhibited a significantly higher incidence of GS bodies than daughter cells, and the
37 frequency of GS body formation increased with increasing replicative cell age. Thus, we find
38 that yeast glutamine synthetase bodies form in a manner strongly dependent on available glucose
39 and increase markedly with cell age.
40
41
42
43
44
45

45 **INTRODUCTION**

46 Evidence is building that protein aggregation *in vivo* may be far more common than
47 expected, with widespread protein aggregation observed in fission yeast cells (Matsuyama et al.
48 2006; Hayashi et al. 2009), in nutritionally or chemically stressed budding yeast cells
49 (Narayanaswamy et al. 2009; Jacobson et al. 2012; Tkach et al. 2012; O'Connell et al. 2014),
50 and in aged nematodes (David et al. 2010), among many other conditions and organisms. Many
51 of these proteins are observed to assemble *in vivo* into large intracellular bodies (O'Connell et al.
52 2012), forming a wide array of intracellular structures, from cytoplasmic dots to domains to oil
53 droplet-like structures. As such, intracellular protein aggregates join a growing array of cellular
54 bodies with differing properties and associated proteins, including nuclear stress bodies
55 (Biamonti 2004), stress granules (Buchan and Parker 2009), actin bodies (Sagot et al. 2006),
56 proteasome bodies (Laporte et al. 2008), aggresomes (Kopito 2000), inclusion bodies (Shively
57 1974), and P-bodies (Ingelfinger et al. 2002), among others (O'Connell et al. 2012). Many of
58 these intracellular bodies, especially those found from high-throughput cell imaging screens,
59 await detailed characterization, and key questions include defining molecular constituents and
60 possible cellular roles, if any, for these various intracellular bodies (Cioce and Lamond 2005;
61 Buckingham and Liu 2011; Biamonti 2004; Cotto, Fox, and Morimoto 1997; Biamonti and
62 Vourc'h 2010; Campbell et al. 2007; Zhao et al. 2013; Xia et al. 2008; Yeates et al. 2008).

63 Among many metabolic enzymes now known to assemble into intracellular bodies
64 (O'Connell et al. 2012), the enzyme glutamine synthetase is notable for serving a key role in
65 central nitrogen metabolism, catalyzing the condensation of glutamate with ammonia to form
66 glutamine. The endogenous *S. cerevisiae* protein (Gln1p) is a 42 kDa enzyme that assembles
67 into a homodecamer (He et al. 2009). The homologous *E. coli* glutamine synthetase forms a
68 dodecamer, and the purified enzyme shows the remarkable property of assembling *in vitro* into
69 fibers through dodecamer-dodecamer stacking interactions (Miller 1974; Dabrowski et al. 1994).
70 Moreover, intracellular *E. coli* glutamine synthetase aggregation is known to be induced *in vivo*
71 by oxidation, preceding its degradation (Smith 1991; Berlett 1997; Bosshard et al. 2010; Levine
72 1981).

73 Recently, it has been shown that a green fluorescent protein fusion to glutamine
74 synthetase expressed in *S. cerevisiae* from the native genomic locus (Gln1-GFP) forms
75 intracellular protein bodies (GS bodies) following various types of nutrient deprivation, chemical
76 stress, or DNA damage (Narayanaswamy et al. 2009; (O'Connell et al. 2014); Tkach et al. 2012).
77 The bodies have been confirmed to form independently of the GFP fusion partner, both through
78 assaying with alternative epitope tags (HA or TAP tags) and through the use of mass
79 spectrometry to confirm that the endogenous untagged protein also forms insoluble protein
80 bodies (Narayanaswamy et al. 2009; O'Connell et al. 2014). GS bodies are not observed to co-
81 localize with major cellular organelles (e.g., nucleus, endoplasmic reticulum, or vacuoles) nor
82 with other canonical intracellular protein bodies, e.g. actin bodies and P-bodies (Narayanaswamy
83 et al. 2009). The bodies survive cell lysis, and mass spectrometry analysis indicates that they are
84 composed almost exclusively of glutamine synthetase and the Hsp90 chaperones Hsp82p and
85 Hsc82p (O'Connell et al. 2014). Gln1p is normally expressed in exponentially growing yeast
86 cells in rich medium at very high levels, approximately 350,000 molecules per cell
87 (Ghaemmaghami et al. 2003), and models such as the "life-on-the-edge" theory would suggest
88 that the protein might be expressed natively close to its limit of solubility during exponential
89 cellular growth (Tartaglia et al. 2007; Ciryam et al. 2013).

90 In order to better understand the *in vivo* conditions that might drive a highly expressed,
91 soluble protein into compact, insoluble protein bodies, we developed a high-throughput single
92 cell assay for GS body formation based on imaging flow cytometry. Using this assay, we
93 quantified the formation of GS bodies in response to available glucose and cell age. In particular,
94 we hypothesized that depleting cellular energy levels would lead to less effective protein
95 homeostasis and a concomitant aggregation of Gln1p. Indeed, GS bodies have been previously
96 observed to form in stationary phase cells as well as in cells transferred into glucose dropout
97 medium (Narayanaswamy et al. 2009)(e.g., as shown in **Figure 1A**). We therefore quantified the
98 kinetic dependence of GS body formation on available glucose and in response to addition of an
99 inhibitor of hexokinase. We find that GS body formation is strongly dependent on glucose, as is
100 the number and size of bodies formed. Treatment with the compound rapamycin, which globally
101 reduces protein synthesis rates and increases levels of autophagy, strongly reduced the incidence
102 of GS bodies. Finally, the tendency to form GS bodies was strongly correlated with replicative
103 aging of the yeast, significantly greater in mother cells than daughter cells, and generally
104 increased with cell size, raising the possibility that the bodies were preferentially formed or
105 retained in mother cells.

106 107 108 **MATERIALS AND METHODS**

109 **Growth and microscopy of yeast**

110 Yeast strains had a genetic background of BY4741 [genotype, MATa his3_1 leu2_0
111 met15_0 ura3_0]. Strains expressing GFP-tagged proteins were obtained from the
112 OpenBiosystems GFP collection. Rich (YPD) medium containing Yeast Extract (1%), Peptone
113 (2%) and glucose (2%) was purchased from Sunrise Sciences. Synthetic complete medium (SC)
114 contained 1x Yeast Nitrogen Base (BD Biosciences/Difco) without amino acids, synthetic drop-
115 out medium supplement mix or was purchased from Sigma. Cultures were started from by
116 picking from freezer stocks into YPD and growing overnight, before transferring to new media
117 for regrowth. Log phase cells were imaged and prepared for mass spec at an O.D. of
118 approximately 2. Stationary phase cells were grown a minimum of 48 hours before imaging or
119 lysing for mass spec analysis. All cultures were maintained shaking at 30°C.

120 For assays in the presence of 2-deoxy glucose, cells in late log phase, defined as an
121 optical density of 2/ml, were spun down, washed with SC-glucose, re-suspended in SC-glucose
122 with 2% 2-deoxyglucose (Sigma) for 2h shaking at 30C.

123 Cells were imaged on a Nikon E800 fluorescence microscope with Photometrix Coolsnap
124 CCD camera under oil immersion at 100x magnification. DIC images and fluorescent images in
125 the GFP channels were collected using standard filter sets. Cell lysate was imaged on a Nikon
126 TE2000-E with a Photometrics Cascade II camera at 60x magnification. Images were processed
127 using Nikon Elements AR.

128 For assessing effects of glucose depletion, cells in early log phase (~2 O.D./ml) were
129 centrifuged and resuspended in SC with glucose concentrations ranging from 0 to 2% (at ~1
130 O.D./ml). At 30 minute or 1 hour intervals, 300µl of culture was removed and fixed by
131 incubation with 4% formaldehyde at room temperature for 60 min, and washed with PBS before
132 storing at 4°C. Cell aliquots were then analyzed using the imaging flow cytometry assay. The
133 change in percent penetrance of GS bodies across each cell population over time was fitted with
134 an allosteric sigmoidal equation to calculate the onset of GS body formation. The time at fifty

135 percent maximum penetrance was plotted against glucose concentration to determine glucose
136 dependence of GS body formation.

137
138 **Imaging flow cytometry for high-throughput quantification of GS body formation**

139 Cells were imaged on an Amnis ImageStream imaging flow cytometer at 60x, collecting both
140 brightfield and GFP fluorescent channels. For each replicate, 50,000 cell images were collected
141 at a flow rate of 40mm/s and a flow width of 7mm. Images were analyzed using Amnis IDEAS
142 4.0 software and custom templates to filter images based on proper focus and cell viability. Cell
143 images were computationally sorted into populations based on foci phenotype and properties of
144 the fluorescence signal. The percentage of cells containing GS bodies was calculated as the
145 proportion of cells with greater than 30% of total cellular GFP fluorescence signal in an area less
146 than approximately $1.25 \mu\text{m}^2$. We observed foci size to scale with integrated fluorescence
147 intensity (F) according to the equation (eqn 1):
148

$$A = \frac{6 \times 10^{-5} \mu\text{m}^2}{\text{relative fluorescence units}} \times F + 1.2 \mu\text{m}^2 \quad (1)$$

150
151 where (F) is the integrated fluorescence intensity of the smallest number of contiguous pixels
152 that account for at least 30% of total cellular fluorescence and (A) is the sum of the area of those
153 pixels.

154
155 **Fluorescence-activated cell sorting and cell imaging**

156 In order to determine the effects of increasing cell age on the formation of GS bodies, we
157 grew cultures of Gln1-GFP yeast to stationary phase in YPD (5 days) and fixed cells as described
158 above. Bud scars on cells were fluorescently marked by incubation for 20 minutes with
159 calcofluor-white (100 $\mu\text{l/ml}$ PBS cell suspension). The brightest 1% of calcofluor-white
160 fluorescent cells were isolated using FACS, resulting in a population enriched for older mother
161 yeast cells. Cells were imaged as described above, additionally monitoring calcofluor-white
162 fluorescence using a standard DAPI filter set to detect the bud scars. To improve bud scar and
163 GS body imaging, 15 μm deep Z-stacks of 3 μm thick slices were captured for each imaged
164 field. Maximum intensity projections were calculated for each Z-stack and, together with the
165 raw data, used to measure cell size (as estimated by cross sectional area at the focal plane),
166 number of bud scars, and count of GS bodies per cell.

167
168 **Quantifying rapamycin effects by imaging flow cytometry**

169 Gln1-GFP yeast cultures were inoculated from frozen cultures and grown to 0.2 OD/ml in
170 SC in triplicate, then subcultured and grown to approximately 1 OD/ml in SC before the addition
171 of rapamycin (Sigma) in DMSO to reach final concentrations of 200, 100, 20, 1, and 0 nM
172 rapamycin (DMSO only; no differences were observed relative to a control sample without
173 DMSO). Cells were grown an additional 30 h until cultures had passed the diauxic shift before
174 fixing with formaldehyde, as described above, and analyzed using the imaging flow cytometry
175 assay.

176

177 **RESULTS AND DISCUSSION**

178 **Formation of GS bodies depends strongly upon available glucose**

179 In order to quantify the formation of GS bodies at the single cell level and across many
180 individual cells, we first developed a high-throughput assay based upon imaging flow cytometry:
181 For a given aliquot of Gln1-GFP expressing yeast cells, the cells are fixed with 4% formaldehyde
182 to prevent potential changes in protein localization prior to analysis, then approximately 50,000
183 cells are individually photographed using imaging flow cytometry and the formation of GS
184 bodies measured on a per cell basis using an automated image analysis pipeline (**Figure 1B**). The
185 assay is thus significantly higher in throughput than manual analysis of standard fluorescence
186 microscopy images, and the correspondingly higher cell counts allow for greater precision and
187 statistical power in quantifying the occurrence of GS body formation across populations of cells.

188 Using this assay, we quantified the extent of GS body formation as a function of available
189 glucose in the growth medium, measuring the frequency of cells exhibiting detectable GS bodies
190 as a function of time and for differing concentrations of glucose in the medium (**Figure 1C**).
191 Gln1-GFP tagged yeast cells growing exponentially in 2% glucose were transferred to medium
192 either lacking glucose altogether, or supplemented with varying glucose concentrations, and cell
193 aliquots were assayed using imaging flow cytometry. We found that decreased glucose
194 concentrations led to a corresponding decrease in the onset time of GS body formation (**Figure**
195 **1C,D**), confirming glucose, or possibly cell energy level, dependence to GS body formation.

196

197 **The count of GS bodies per cell also depends upon available glucose levels**

198 In the above assays, the frequency of cells forming GS bodies clearly depended upon
199 glucose levels. We further examined the count of GS bodies per cell to determine if the count
200 varied on a cell-to-cell basis. Notably, the majority of cells transferred into glucose dropout
201 medium formed one or two large GS bodies (**Figure 2**), as, for example, can be seen in the cell
202 images of **Figure 1A**.

203 However, when Gln1-GFP tagged yeast cells were subcultured into growth medium both
204 lacking glucose and containing 2-deoxyglucose (2DG), a competitive inhibitor of hexokinase,
205 many small foci formed per cell rather than one or two large foci, as commonly seen in glucose
206 depletion alone (**Figures 1A, 2**). Thus, GS body population penetrance and count per cell show
207 dependencies on available glucose and hexokinase activity, respectively. One possibility may be
208 that GS bodies form initially as numerous small foci that must coalesce into one or two large
209 foci; for example, one mechanism involving active transport is required to establish aggresomes
210 (Johnston, Ward, and Kopito 1998; Muchowski et al. 2002). Alternatively, 2DG treatment may
211 simply affect other steps required for large GS body formation.

212

213 **Rapamycin treatment markedly reduces GS body formation**

214 Because GS body formation increases with stress and decreases with metabolic activity,
215 we speculated that rapamycin treatment might reduce GS body formation. Within cells,
216 rapamycin binds to Frp1p, which in turn inhibits the TOR Complex 1 (TORC1)(Stan et al. 1994;
217 Choi et al. 1996). Following TORC1 inhibition, cells behave as if starved, arresting division in
218 G₀ (Cardenas et al. 1999) and releasing the repression of autophagy and the Msn2/Msn4-
219 mediated stress response pathways (Kamada et al. 2000; Monteiro and Netto 2004). Rapamycin
220 also decreases translation initiation and ribosome biogenesis, collectively decreasing the steady-
221 state protein concentration inside cells (Martin, Soulard, and Hall 2004). These mechanisms thus

222 directly affect cellular processes related to stress, aging, and aggregation in a manner that we
223 might expect to reduce GS body formation.

224 In order to test this hypothesis, we grew Gln1-GFP tagged yeast in a range concentrations
225 of the drug spanning 2 orders of magnitude for 24 hours. Using the imaging flow cytometry
226 assay, we found a clear dose-dependent reduction in GS body formation in response to
227 rapamycin treatment, with half maximal population penetrance of GS body formation occurring
228 in response to treatment with approximately 1 nM rapamycin (**Figure 3B**). Only a small
229 proportion of cells exhibited GS bodies upon treatment with 20 nM or higher rapamycin doses
230 (e.g., **Figure 3A**). Notably, many specific cellular mechanisms might contribute to this
231 reduction, including both the decreased cellular protein levels increased autophagy known to
232 follow rapamycin treatment.

233

234 **GS bodies form at higher rates in replicatively older cells**

235 Many of the mechanisms that cells use to contain and clear protein aggregates are known
236 to decline in efficacy with age across a variety of organisms. Chaperone expression decreases
237 (Lund et al. 2002), proteasome activity diminishes (Tonoki et al. 2009), and chaperone-mediated
238 autophagy slows with increasing cellular and organismal age (Cuervo and Dice 2000), among
239 other trends. This phenomenon potentially contributes to the accumulation of aggregation in age-
240 related diseases, such as plaques in Alzheimer's disease (Morimoto and Cuervo 2009). Recent
241 work in nematodes has shown that widespread protein aggregation occurs normally in the course
242 of aging (David et al. 2010). Given such associations between aging and protein aggregation, and
243 given our observed reduction of GS body formation by rapamycin treatment, we therefore next
244 asked if GS body formation correlated with cell age. Two easily assayable proxies of replicative
245 age in yeast are an expansion of cell volume (Pichová, Vondráková, and Breitenbach 1997) and
246 the accompanying accumulation of bud scars with each replicative cycle (Mortimer and Johnston
247 1959; Müller et al. 1980).

248 We observed a clear correlation between the frequency of GS body formation and
249 measured cell diameter, as assayed using fluorescence microscopy (Pearson $r^2 = 0.78$; **Figure**
250 **4A**). To obtain an independent assay of cell size, we isolated the largest and smallest 5 percent
251 of yeast cells using low-angle forward scattering fluorescence activated cell sorting (FACS), then
252 imaged the cells by fluorescence microscopy, manually measuring cell diameter and scoring the
253 occurrence of GS bodies. This assay confirmed the same general trend ($p \leq 10^{-4}$; **Figure 4B**).

254 Due to exponential growth, any mixed population of yeast cells is dominated by young
255 cells, with old cells found only rarely. Thus, in order to directly estimate replicative age by
256 measuring the accumulation of bud scars, we first enriched for yeast cells that had undergone
257 more replicative budding cycles *via* the use of FACS on the basis of the fluorescent bud scar
258 marker dye calcofluor-white. We then imaged the sorted cells using fluorescence microscopy
259 and directly counted both bud scars and GS bodies per cell (e.g., as in **Figure 5A**).

260 The frequency of cells with GS bodies increased steadily with cell age, as measured by
261 bud scar count, from a base rate of ~76% in unbudded cells and saturating at approx. 95% of the
262 population among cells with 10 or more bud scars (**Figure 5B**). Moreover, cells with more bud
263 scars were found to be more likely to contain a higher count of GS bodies per cell (though the
264 correlation was not linear) with the largest increase in the mean number of GS bodies per cell
265 occurring between cells with no bud scars and cells with one bud scar (**Figure 5C**). The
266 difference was more marked when we narrowed the analysis strictly to pairs of mother and
267 daughter cells that had yet to undergo cell separation. Mother cells were significantly more likely

268 to contain GS bodies than their connected daughter cells, and also to exhibit higher counts of GS
269 bodies per cell ($p \leq 10^{-10}$; **Figure 5D**), suggesting the possibility that mother cells might
270 preferentially retain GS bodies, a hallmark of replicative aging in yeast cells for senescence
271 factors (Aguilaniu et al. 2003)(Kaeberlein 2010).
272
273

274 CONCLUSIONS

275 In summary, we describe a high-throughput single cell assay for the formation of
276 intracellular protein bodies by the metabolic enzyme glutamine synthetase. Using this assay, we
277 demonstrate that reduced glucose availability or the addition of a hexokinase inhibitor both
278 strongly induce GS body formation; the latter also increases the count and decreases the size of
279 the GS bodies formed. The formation of GS bodies increased both with increasing cell age and
280 cell size; in contrast, treatment with the drug rapamycin suppressed GS body formation. Thus,
281 GS body formation depends strongly both upon available glucose levels and replicative cell age.
282
283
284

285 ACKNOWLEDGEMENTS

286 We would like to acknowledge Drs. Angela Bardo and Gwen Stovall for assistance with imaging
287 flow cytometry, Dr. Richard Salinas of the ICMB core facility for his assistance with FACS, and
288 Dr. Andrew Ellington for numerous helpful discussions. This work was supported by grants from
289 the National Institutes of Health, National Science Foundation, Cancer Prevention Research
290 Institute of Texas, and the Welch (F1515) Foundation to EMM. MT acknowledges funding and
291 support from Michele Vendruscolo and the University of Cambridge.
292

293

293 **REFERENCES**

294

295 Aguilaniu, Hugo, Lena Gustafsson, Michel Rigoulet, and Thomas Nyström. 2003. “Asymmetric
296 Inheritance of Oxidatively Damaged Proteins during Cytokinesis.” *Science (New York,*
297 *N.Y.)* 299 (5613): 1751–3. doi:10.1126/science.1080418.
298 <http://www.ncbi.nlm.nih.gov/pubmed/12610228>.

299 Berlett, B. S. 1997. “Protein Oxidation in Aging, Disease, and Oxidative Stress.” *Journal of*
300 *Biological Chemistry* 272 (33) (August 15): 20313–20316. doi:10.1074/jbc.272.33.20313.
301 <http://www.jbc.org.ezproxy.lib.utexas.edu/content/272/33/20313.short>.

302 Biamonti, Giuseppe. 2004. “Nuclear Stress Bodies: A Heterochromatin Affair?” *Nature Reviews.*
303 *Molecular Cell Biology* 5 (6) (June): 493–8. doi:10.1038/nrm1405.
304 <http://dx.doi.org/10.1038/nrm1405>.

305 Biamonti, Giuseppe, and Claire Vourc’h. 2010. “Nuclear Stress Bodies.” *Cold Spring Harbor*
306 *Perspectives in Biology* 2 (6): a000695. doi:10.1101/cshperspect.a000695.
307 [http://www.pubmedcentral.nih.gov/articlerender.fcgi?artid=2869524&tool=pmcentrez&ren](http://www.pubmedcentral.nih.gov/articlerender.fcgi?artid=2869524&tool=pmcentrez&rendertype=abstract)
308 [dertype=abstract](http://www.pubmedcentral.nih.gov/articlerender.fcgi?artid=2869524&tool=pmcentrez&rendertype=abstract).

309 Bosshard, Franziska, Kathrin Riedel, Thomas Schneider, Carina Geiser, Margarete Bucheli, and
310 Thomas Egli. 2010. “Protein Oxidation and Aggregation in UVA-Irradiated Escherichia
311 Coli Cells as Signs of Accelerated Cellular Senescence.” *Environmental Microbiology* 12
312 (11) (November): 2931–45. doi:10.1111/j.1462-2920.2010.02268.x.
313 <http://www.ncbi.nlm.nih.gov/pubmed/20545749>.

314 Buchan, J Ross, and Roy Parker. 2009. “Eukaryotic Stress Granules: The Ins and Outs of
315 Translation.” *Molecular Cell* 36 (6) (December 25): 932–41.
316 doi:10.1016/j.molcel.2009.11.020. <http://dx.doi.org/10.1016/j.molcel.2009.11.020>.

317 Buckingham, Mickey, and Ji-Long Liu. 2011. “U Bodies Respond to Nutrient Stress in
318 Drosophila.” *Experimental Cell Research* 317 (20): 2835–2844.
319 doi:10.1016/j.yexcr.2011.09.001. <http://www.ncbi.nlm.nih.gov/pubmed/21939654>.

320 Campbell, Edward M, Mark P Dodding, Melvyn W Yap, Xiaolu Wu, Sarah Gallois-Montbrun,
321 Michael H Malim, Jonathan P Stoye, and Thomas J Hope. 2007. “TRIM5 Alpha
322 Cytoplasmic Bodies Are Highly Dynamic Structures.” *Molecular Biology of the Cell* 18 (6):
323 2102–11. doi:10.1091/mbc.E06-12-1075. <http://www.ncbi.nlm.nih.gov/pubmed/17392513>.

324 Cardenas, M E, N S Cutler, M C Lorenz, C J Di Como, and J Heitman. 1999. “The TOR
325 Signaling Cascade Regulates Gene Expression in Response to Nutrients.” *Genes &*
326 *Development* 13 (24) (December 15): 3271–9.

- 327 <http://www.pubmedcentral.nih.gov/articlerender.fcgi?artid=317202&tool=pmcentrez&rendertype=abstract>.
328
- 329 Choi, J, J Chen, S L Schreiber, and J Clardy. 1996. "Structure of the FKBP12-Rapamycin
330 Complex Interacting with the Binding Domain of Human FRAP." *Science (New York, N.Y.)*
331 273 (5272) (July 12): 239–42. <http://www.ncbi.nlm.nih.gov/pubmed/8662507>.
- 332 Cioce, Mario, and Angus I Lamond. 2005. "Cajal Bodies: A Long History of Discovery." *Annual*
333 *Review of Cell and Developmental Biology* 21 (January 7): 105–31.
334 doi:10.1146/annurev.cellbio.20.010403.103738.
335 <http://www.annualreviews.org/doi/abs/10.1146/annurev.cellbio.20.010403.103738>.
- 336 Ciryam, Prajwal, Gian Gaetano Tartaglia, Richard I Morimoto, Christopher M Dobson, and
337 Michele Vendruscolo. 2013. "Widespread Aggregation and Neurodegenerative Diseases
338 Are Associated with Supersaturated Proteins." *Cell Reports* (October 30).
339 doi:10.1016/j.celrep.2013.09.043.
340 <http://www.sciencedirect.com/science/article/pii/S2211124713005664>.
- 341 Cotto, J, S Fox, and R Morimoto. 1997. "HSF1 Granules: A Novel Stress-Induced Nuclear
342 Compartment of Human Cells." *Journal of Cell Science* 110 (Pt 2: 2925–2934.
343 <http://www.ncbi.nlm.nih.gov/pubmed/9359875>.
- 344 Cuervo, A M, and J F Dice. 2000. "Age-Related Decline in Chaperone-Mediated Autophagy."
345 *The Journal of Biological Chemistry* 275 (40) (October 6): 31505–13.
346 doi:10.1074/jbc.M002102200. <http://www.ncbi.nlm.nih.gov/pubmed/10806201>.
- 347 Dabrowski, M J, J Yanchunas, B C Villafranca, E C Dietze, P Schurke, and W M Atkins. 1994.
348 "Supramolecular Self-Assembly of Glutamine Synthetase: Mutagenesis of a Novel
349 Intermolecular Metal Binding Site Required for Dodecamer Stacking." *Biochemistry* 33
350 (50) (December 20): 14957–64. <http://www.ncbi.nlm.nih.gov/pubmed/7999751>.
- 351 David, Della C, Noah Ollikainen, Jonathan C Trinidad, Michael P Cary, Alma L Burlingame,
352 and Cynthia Kenyon. 2010. "Widespread Protein Aggregation as an Inherent Part of Aging
353 in *C. Elegans*." *PLoS Biology* 8 (8) (January): e1000450. doi:10.1371/journal.pbio.1000450.
354 <http://www.pubmedcentral.nih.gov/articlerender.fcgi?artid=2919420&tool=pmcentrez&rendertype=abstract>.
355
- 356 Ghaemmaghami, Sina, Won-Ki Huh, Kiowa Bower, Russell W Howson, Archana Belle, Noah
357 Dephoure, Erin K O'Shea, and Jonathan S Weissman. 2003. "Global Analysis of Protein
358 Expression in Yeast." *Nature* 425 (6959) (October 16): 737–41. doi:10.1038/nature02046.
359 <http://www.ncbi.nlm.nih.gov/pubmed/14562106>.
- 360 Hayashi, Aki, Da-Qiao Ding, Ding Da-Qiao, Chihiro Tsutsumi, Yuji Chikashige, Hirohisa
361 Masuda, Tokuko Haraguchi, and Yasushi Hiraoka. 2009. "Localization of Gene Products
362 Using a Chromosomally Tagged GFP-Fusion Library in the Fission Yeast

- 363 Schizosaccharomyces Pombe.” *Genes to Cells* 14 (2) (February): 217–25.
364 doi:10.1111/j.1365-2443.2008.01264.x. <http://www.ncbi.nlm.nih.gov/pubmed/19170768>.
- 365 He, Yong-Xing, Long Gui, Yin-Zi Liu, Yang Du, Yeyun Zhou, Ping Li, and Cong-Zhao Zhou.
366 2009. “Crystal Structure of Saccharomyces Cerevisiae Glutamine Synthetase Gln1 Suggests
367 a Nanotube-like Supramolecular Assembly.” *Proteins* 76 (1) (July): 249–54.
368 doi:10.1002/prot.22403. <http://www.ncbi.nlm.nih.gov/pubmed/19322816>.
- 369 Ingelfinger, Dierk, Donna J Arndt-Jovin, Reinhard Lührmann, and Tilmann Achsel. 2002. “The
370 Human LSm1-7 Proteins Colocalize with the mRNA-Degrading Enzymes Dcp1/2 and Xrnl
371 in Distinct Cytoplasmic Foci.” *RNA (New York, N.Y.)* 8 (12) (December): 1489–501.
372 [http://www.pubmedcentral.nih.gov/articlerender.fcgi?artid=1370355&tool=pmcentrez&ren
373 dertype=abstract](http://www.pubmedcentral.nih.gov/articlerender.fcgi?artid=1370355&tool=pmcentrez&rendertype=abstract).
- 374 Jacobson, Therese, Clara Navarrete, Sandeep K Sharma, Theodora C Sideri, Sebastian Ibstedt,
375 Smriti Priya, Chris M Grant, Philipp Christen, Pierre Goloubinoff, and Markus J Tamás.
376 2012. “Arsenite Interferes with Protein Folding and Triggers Formation of Protein
377 Aggregates in Yeast.” *Journal of Cell Science* 125 (Pt 21) (November 1): 5073–83.
378 doi:10.1242/jcs.107029. <http://www.ncbi.nlm.nih.gov/pubmed/22946053>.
- 379 Johnston, J A, C L Ward, and R R Kopito. 1998. “Aggresomes: A Cellular Response to
380 Misfolded Proteins.” *The Journal of Cell Biology* 143 (7) (December 28): 1883–98.
381 <http://www.citeulike.org/user/jdoconnell/tag/aggregation>.
- 382 Kaeberlein, Matt. 2010. “Lessons on Longevity from Budding Yeast.” *Nature* 464 (7288)
383 (March 25): 513–9. doi:10.1038/nature08981.
384 [http://www.nature.com.ezproxy.lib.utexas.edu/nature/journal/v464/n7288/full/nature08981.
385 html](http://www.nature.com.ezproxy.lib.utexas.edu/nature/journal/v464/n7288/full/nature08981.html).
- 386 Kamada, Y, T Funakoshi, T Shintani, K Nagano, M Ohsumi, and Y Ohsumi. 2000. “Tor-
387 Mediated Induction of Autophagy via an Apg1 Protein Kinase Complex.” *The Journal of
388 Cell Biology* 150 (6) (September 18): 1507–13.
389 [http://www.pubmedcentral.nih.gov/articlerender.fcgi?artid=2150712&tool=pmcentrez&ren
390 dertype=abstract](http://www.pubmedcentral.nih.gov/articlerender.fcgi?artid=2150712&tool=pmcentrez&rendertype=abstract).
- 391 Kopito, Ron R. 2000. “Aggresomes, Inclusion Bodies and Protein Aggregation.” *Trends in Cell
392 Biology* 10 (12) (December): 524–530. doi:10.1016/S0962-8924(00)01852-3.
393 <http://linkinghub.elsevier.com/retrieve/pii/S0962892400018523>.
- 394 Laporte, Damien, Bénédicte Salin, Bertrand Daignan-Fornier, and Isabelle Sagot. 2008.
395 “Reversible Cytoplasmic Localization of the Proteasome in Quiescent Yeast Cells.” *The
396 Journal of Cell Biology* 181 (5): 737–45. doi:10.1083/jcb.200711154.
397 <http://www.ncbi.nlm.nih.gov/pubmed/18504300>.

- 398 Levine, R. L. 1981. "Turnover of Bacterial Glutamine Synthetase: Oxidative Inactivation
399 Precedes Proteolysis." *Proceedings of the National Academy of Sciences* 78 (4) (April 1):
400 2120–2124. doi:10.1073/pnas.78.4.2120. <http://www.pnas.org/content/78/4/2120.short>.
- 401 Lund, James, Patricia Tedesco, Kyle Duke, John Wang, Stuart K Kim, and Thomas E Johnson.
402 2002. "Transcriptional Profile of Aging in *C. Elegans*." *Current Biology : CB* 12 (18)
403 (September 17): 1566–73. <http://www.ncbi.nlm.nih.gov/pubmed/12372248>.
- 404 Martin, Dietmar E, Alexandre Soulard, and Michael N Hall. 2004. "TOR Regulates Ribosomal
405 Protein Gene Expression via PKA and the Forkhead Transcription Factor FHL1." *Cell* 119
406 (7) (December 29): 969–79. doi:10.1016/j.cell.2004.11.047.
407 <http://www.ncbi.nlm.nih.gov/pubmed/15620355>.
- 408 Matsuyama, Akihisa, Ritsuko Arai, Yoko Yashiroda, Atsuko Shirai, Ayako Kamata, Shigeko
409 Sekido, Yumiko Kobayashi, et al. 2006. "ORFeome Cloning and Global Analysis of Protein
410 Localization in the Fission Yeast *Schizosaccharomyces Pombe*." *Nature Biotechnology* 24
411 (7) (July): 841–7. doi:10.1038/nbt1222. <http://dx.doi.org/10.1038/nbt1222>.
- 412 Miller, R. 1974. "Zinc-Induced Paracrystalline Aggregation of Glutamine Synthetase." *Archives*
413 *of Biochemistry and Biophysics* 163 (1) (July): 155–171. doi:10.1016/0003-9861(74)90465-
414 2. [http://dx.doi.org/10.1016/0003-9861\(74\)90465-2](http://dx.doi.org/10.1016/0003-9861(74)90465-2).
- 415 Monteiro, Gisele, and Luis Eduardo Soares Netto. 2004. "Glucose Repression of PRX1
416 Expression Is Mediated by Tor1p and Ras2p through Inhibition of Msn2/4p in
417 *Saccharomyces Cerevisiae*." *FEMS Microbiology Letters* 241 (2) (December 15): 221–8.
418 doi:10.1016/j.femsle.2004.10.024. <http://www.ncbi.nlm.nih.gov/pubmed/15598536>.
- 419 Morimoto, Richard I, and Ana M Cuervo. 2009. "Protein Homeostasis and Aging: Taking Care
420 of Proteins from the Cradle to the Grave." *The Journals of Gerontology. Series A,*
421 *Biological Sciences and Medical Sciences* 64 (2) (February): 167–70.
422 doi:10.1093/gerona/gln071.
423 [http://www.pubmedcentral.nih.gov/articlerender.fcgi?artid=2655025&tool=pmcentrez&ren](http://www.pubmedcentral.nih.gov/articlerender.fcgi?artid=2655025&tool=pmcentrez&rendertype=abstract)
424 [dertype=abstract](http://www.pubmedcentral.nih.gov/articlerender.fcgi?artid=2655025&tool=pmcentrez&rendertype=abstract).
- 425 Mortimer, K., and J R Johnston. 1959. "Life Span of Individual Yeast Cells." *Nature* 183 (4677)
426 (June 20): 1751–2. <http://www.ncbi.nlm.nih.gov/pubmed/13666896>.
- 427 Muchowski, Paul J, Ke Ning, Crislyn D'Souza-Schorey, and Stanley Fields. 2002. "Requirement
428 of an Intact Microtubule Cytoskeleton for Aggregation and Inclusion Body Formation by a
429 Mutant Huntingtin Fragment." *Proceedings of the National Academy of Sciences of the*
430 *United States of America* 99 (2) (January): 727–732. doi:10.1073/pnas.022628699.
431 [http://www.pubmedcentral.nih.gov/articlerender.fcgi?artid=117373&tool=pmcentrez&rend](http://www.pubmedcentral.nih.gov/articlerender.fcgi?artid=117373&tool=pmcentrez&rendertype=abstract)
432 [ertype=abstract](http://www.pubmedcentral.nih.gov/articlerender.fcgi?artid=117373&tool=pmcentrez&rendertype=abstract).

- 433 Müller, I, M Zimmermann, D Becker, and M Flömer. 1980. "Calendar Life Span versus Budding
434 Life Span of *Saccharomyces Cerevisiae*." *Mechanisms of Ageing and Development* 12 (1)
435 (January): 47–52. <http://www.ncbi.nlm.nih.gov/pubmed/6986516>.
- 436 Narayanaswamy, Rammohan, Matthew Levy, Mark Tsechansky, Gwendolyn M Stovall, Jeremy
437 D O'Connell, Jennifer Mirrieles, Andrew D Ellington, and Edward M Marcotte. 2009.
438 "Widespread Reorganization of Metabolic Enzymes into Reversible Assemblies upon
439 Nutrient Starvation." *Proceedings of the National Academy of Sciences of the United States*
440 *of America* 106 (25) (June 23): 10147–52. doi:10.1073/pnas.0812771106.
441 <http://www.pnas.org/cgi/content/abstract/106/25/10147>.
- 442 O'Connell, Jeremy D, Mark Tsechansky, Ariel Royall, Daniel R Boutz, Andrew D Ellington,
443 and Edward M Marcotte. 2014. "A Proteomic Survey of Widespread Protein Aggregation in
444 Yeast." *Molecular bioSystems* (February 3). doi:10.1039/c3mb70508k.
445 <http://pubs.rsc.org/en/content/articlehtml/2014/mb/c3mb70508k>.
- 446 O'Connell, Jeremy D., Alice Zhao, Andrew D. Ellington, and Edward M. Marcotte. 2012.
447 "Dynamic Reorganization of Metabolic Enzymes into Intracellular Bodies." *Annual Review*
448 *of Cell and Developmental Biology* 28 (January 11): 89–111. doi:10.1146/annurev-cellbio-
449 101011-155841. [http://www.annualreviews.org/doi/abs/10.1146/annurev-cellbio-101011-
450 155841](http://www.annualreviews.org/doi/abs/10.1146/annurev-cellbio-101011-155841).
- 451 Pichová, A, D Vondráková, and M Breitenbach. 1997. "Mutants in the *Saccharomyces*
452 *Cerevisiae* RAS2 Gene Influence Life Span, Cytoskeleton, and Regulation of Mitosis."
453 *Canadian Journal of Microbiology* 43 (8) (August): 774–81.
454 <http://www.ncbi.nlm.nih.gov/pubmed/9304788>.
- 455 Sagot, Isabelle, Benoît Pinson, Bénédicte Salin, and Bertrand Daignan-Fornier. 2006. "Actin
456 Bodies in Yeast Quiescent Cells: An Immediately Available Actin Reserve?" *Molecular*
457 *Biology of the Cell* 17 (11) (November): 4645–55. doi:10.1091/mbc.E06-04-0282.
458 [http://www.pubmedcentral.nih.gov/articlerender.fcgi?artid=1635378&tool=pmcentrez&ren
459 dertype=abstract](http://www.pubmedcentral.nih.gov/articlerender.fcgi?artid=1635378&tool=pmcentrez&rendertype=abstract).
- 460 Shively, J M. 1974. "Inclusion Bodies of Prokaryotes." *Annual Review of Microbiology* 28
461 (January): 167–87. doi:10.1146/annurev.mi.28.100174.001123.
462 <http://www.ncbi.nlm.nih.gov/pubmed/4372937>.
- 463 Smith, C. D. 1991. "Excess Brain Protein Oxidation and Enzyme Dysfunction in Normal Aging
464 and in Alzheimer Disease." *Proceedings of the National Academy of Sciences* 88 (23)
465 (December 1): 10540–10543. doi:10.1073/pnas.88.23.10540.
466 <http://www.pnas.org.ezproxy.lib.utexas.edu/content/88/23/10540.short>.
- 467 Stan, R, M M McLaughlin, R Cafferkey, R K Johnson, M Rosenberg, and G P Livi. 1994.
468 "Interaction between FKBP12-Rapamycin and TOR Involves a Conserved Serine Residue."
469 *The Journal of Biological Chemistry* 269 (51) (December 23): 32027–30.
470 <http://www.ncbi.nlm.nih.gov/pubmed/7528205>.

- 471 Tartaglia, Gian Gaetano, Sebastian Pechmann, Christopher M Dobson, and Michele
472 Vendruscolo. 2007. "Life on the Edge: A Link between Gene Expression Levels and
473 Aggregation Rates of Human Proteins." *Trends in Biochemical Sciences* 32 (5) (May): 204–
474 6. doi:10.1016/j.tibs.2007.03.005. <http://www.ncbi.nlm.nih.gov/pubmed/17419062>.
- 475 Tkach, Johnny M, Askar Yimit, Anna Y Lee, Michael Riffle, Michael Costanzo, Daniel Jaschob,
476 Jason A Hendry, et al. 2012. "Dissecting DNA Damage Response Pathways by Analysing
477 Protein Localization and Abundance Changes during DNA Replication Stress." *Nature Cell
478 Biology* 14 (9) (September): 966–76. doi:10.1038/ncb2549.
479 [http://www.pubmedcentral.nih.gov/articlerender.fcgi?artid=3434236&tool=pmcentrez&ren
480 dertype=abstract](http://www.pubmedcentral.nih.gov/articlerender.fcgi?artid=3434236&tool=pmcentrez&rendertype=abstract).
- 481 Tonoki, Ayako, Erina Kuranaga, Takeyasu Tomioka, Jun Hamazaki, Shigeo Murata, Keiji
482 Tanaka, and Masayuki Miura. 2009. "Genetic Evidence Linking Age-Dependent
483 Attenuation of the 26S Proteasome with the Aging Process." *Molecular and Cellular
484 Biology* 29 (4) (February 15): 1095–106. doi:10.1128/MCB.01227-08.
485 <http://mcb.asm.org/content/29/4/1095.short>.
- 486 Xia, Qiangwei, Lujian Liao, Dongmei Cheng, Duc M Duong, Marla Gearing, James J Lah, Allan
487 I Levey, and Junmin Peng. 2008. "Proteomic Identification of Novel Proteins Associated
488 with Lewy Bodies." *Frontiers in Bioscience: A Journal and Virtual Library* 13 (January):
489 3850–6.
490 [http://www.pubmedcentral.nih.gov/articlerender.fcgi?artid=2663966&tool=pmcentrez&ren
491 dertype=abstract](http://www.pubmedcentral.nih.gov/articlerender.fcgi?artid=2663966&tool=pmcentrez&rendertype=abstract).
- 492 Yeates, Todd O, Cheryl A Kerfeld, Sabine Heinhorst, Gordon C Cannon, and Jessup M Shively.
493 2008. "Protein-Based Organelles in Bacteria: Carboxysomes and Related
494 Microcompartments." *Nature Reviews. Microbiology* 6 (9) (September 4): 681–91.
495 doi:10.1038/nrmicro1913. <http://dx.doi.org/10.1038/nrmicro1913>.
- 496 Zhao, Alice, Mark Tsechansky, Jagannath Swaminathan, Lindsey Cook, Andrew D. Ellington,
497 and Edward M. Marcotte. 2013. "Transiently Transfected Purine Biosynthetic Enzymes
498 Form Stress Bodies." *PloS One* 8 (2) (January): e56203. doi:10.1371/journal.pone.0056203.
499 [http://www.pubmedcentral.nih.gov/articlerender.fcgi?artid=3566086&tool=pmcentrez&ren
500 dertype=abstract](http://www.pubmedcentral.nih.gov/articlerender.fcgi?artid=3566086&tool=pmcentrez&rendertype=abstract).

501

502

503

503 **FIGURE LEGENDS**

504 **Figure 1. Intracellular Gln1-GFP protein bodies form in a manner dependent on glucose**
505 **availability.**

506 (A) As assayed by fluorescence microscopy, Gln1-GFP tagged yeast strains in log phase growth
507 exhibit visible foci (GS bodies) when starved for glucose either by removal of glucose from the
508 growth medium or by addition of a non-metabolizable competitive inhibitor, 2-deoxyglucose.

509 (B) Schematic view of GS body counting workflow. Approximately 50,000 individual yeast cells
510 are imaged per sample on an Amnis ImageStream; cell images are then processed automatically
511 to select in-focus, individual cells with measurable GFP fluorescence. Cells that pass these filters
512 are analyzed for the intensity and size of the 30% intensity mask, which classifies cells into GS
513 body and non-GS body containing populations. (C) Quantifying GS body formation over time
514 across a range of range of glucose concentrations indicates that reducing glucose available in the
515 growth medium significantly enhances the onset of GS body formation. (D) Plotting the
516 concentration of glucose for a yeast culture against the time to 50% population penetrance
517 reveals a marked correlation between available glucose and the rate of GS body formation.

518
519 **Figure 2. Inhibition of glycolysis induces higher numbers of GS bodies per cell.**

520 Removal of glucose from the growth medium slows and eventually halts glycolysis as residual
521 glucose is depleted, and leads to strong induction of one or two visible foci per cell after 2h.

522 Direct inhibition of glycolysis by the addition of a competitive inhibitor of glucose hexokinase,
523 2-deoxyglucose (2DG; added at 2%), induces formation of many small foci rather than one or
524 two large foci, suggesting that the assembly of one or two large foci per cell may be an energy
525 dependent process.

526 **Figure 3. Rapamycin treatment strongly reduces the population penetrance of GS bodies.**

527 A) Widefield fluorescent microscopy images illustrating the marked decrease in GS body
528 formation following rapamycin treatment. B) The proportions of cells exhibiting visible GS
529 bodies were measured in an unbiased fashion by automatically imaging cells at high-throughput
530 using imaging flow cytometry, identifying and quantifying the relevant cell subpopulations as
531 shown. Rapamycin treatment induced a dose-dependent reduction in the proportions of cells with
532 GS bodies across a concentration range of 1 to 200 nM.

533 **Figure 4. GS body formation correlates with cell size, a proxy for cell age.**

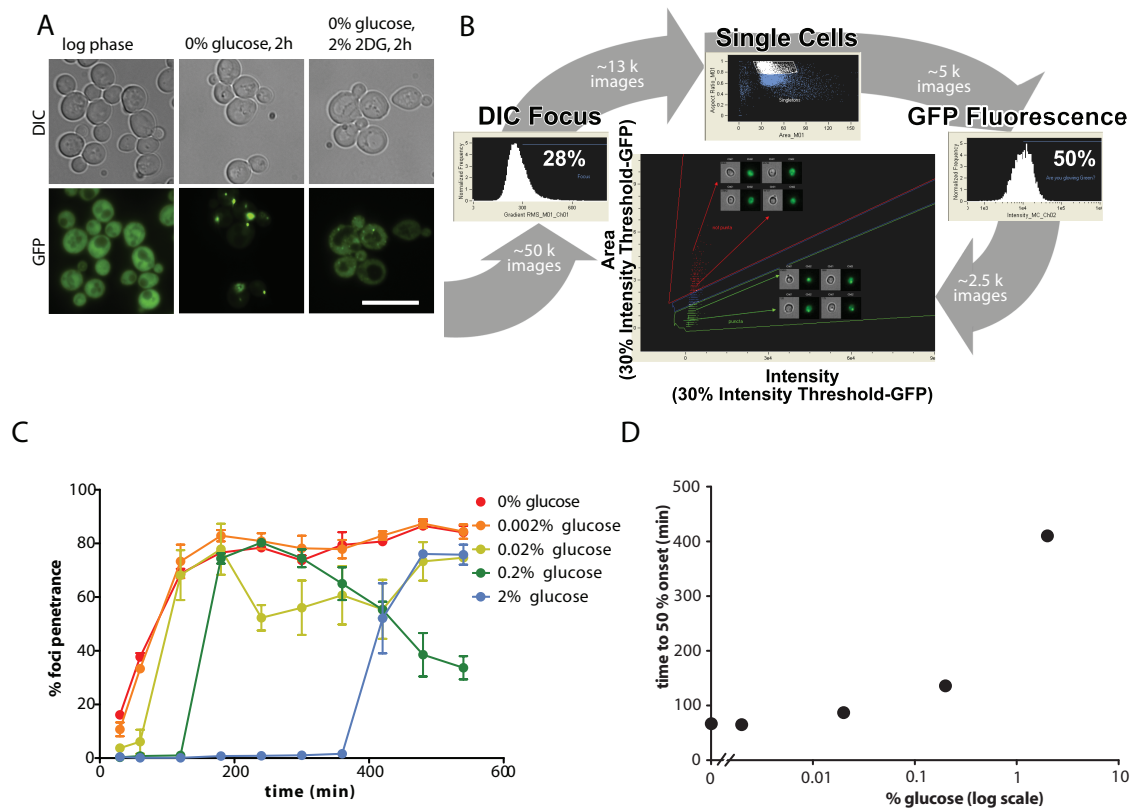
534 A) Increasing cell size is a proxy marker for age, and positively correlates with the likelihood of
535 having GS bodies, as measured by fluorescence microscopy (Pearson $r^2=0.78$; $n = 100$ cells). B)
536 GS bodies form at higher rates in larger cells, as assayed by fluorescence activated cell sorting
537 (FACS) yeast cells by size and manually scoring GS bodies ($p \leq 10^{-4}$; $n = 100$ cells).

538 **Figure 5. GS body formation increases with replicative age and occurs more frequently in**
539 **mother cells than daughter cells.**

540 A) Maximum intensity projection of a z-stack of widefield fluorescence microscopy images of
541 calcofluor white stained Gln1-GFP expressing cells B) Cells with more bud scars show a higher
542 incidence of GS bodies and C) have higher counts of GS bodies per cell (ANOVA, $p \leq 10^{-4}$), as
543 measured for yeast cells FACS sorted on the basis of the fluorescent bud scar dye calcofluor
544 white, manually counting the number of budscars and GS bodies per cell. Notably, the
545 population penetrance of GS body incidence rises significantly with age. In contrast, the count of
546 GS bodies per cell, which rises between unbudded cells and cells with 1 or more bud scars,
547 shows no significant dependence on replicative age after the first budding. D) In order to directly
548 quantify the formation of GS bodies in new buds relative to their mothers, we reanalyzed the

549 data in (B) focusing only on the subset of cell images with mother and daughter cells still
550 connected, as diagrammed in the figure. Mother cells were more likely both to have GS bodies
551 and to exhibit multiple GS bodies than their own reproductively *naïve* daughters (Mann-Whitney
552 U test, $p \leq 10^{-10}$).

553
554
555



556

557

558

559

560

561

562

563

564

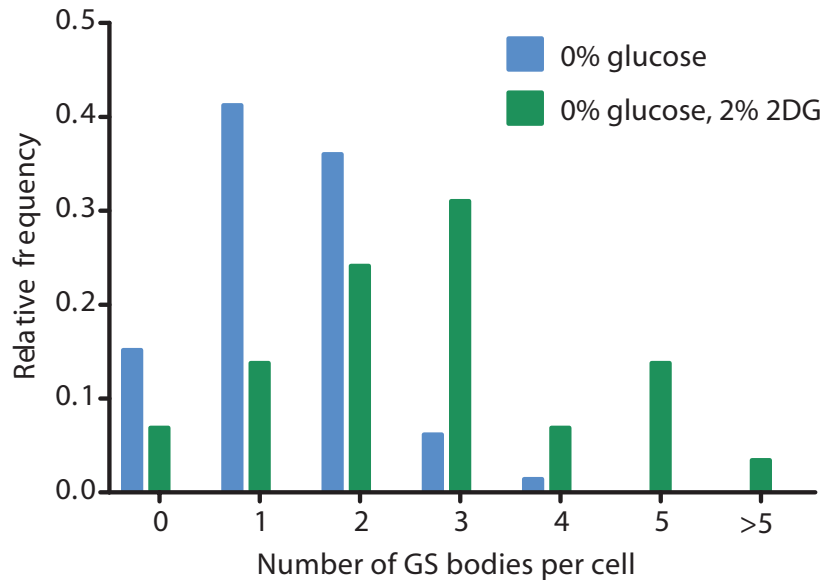
565 **Figure 1**

566

566

567

568



569

570

571

572

573

574

575

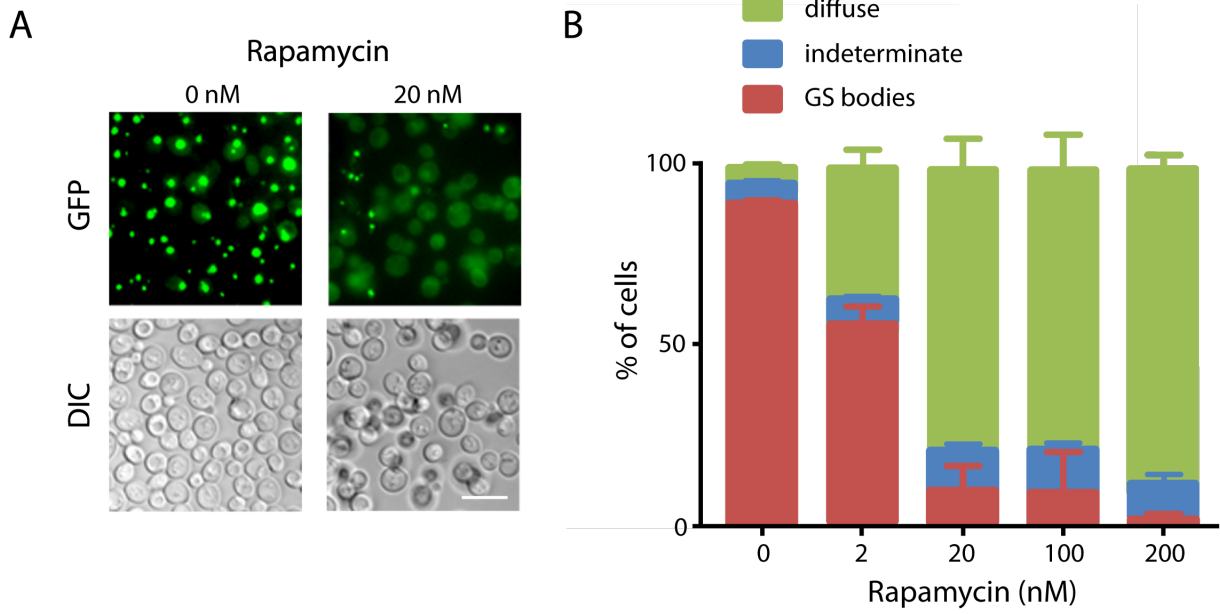
576

577

578

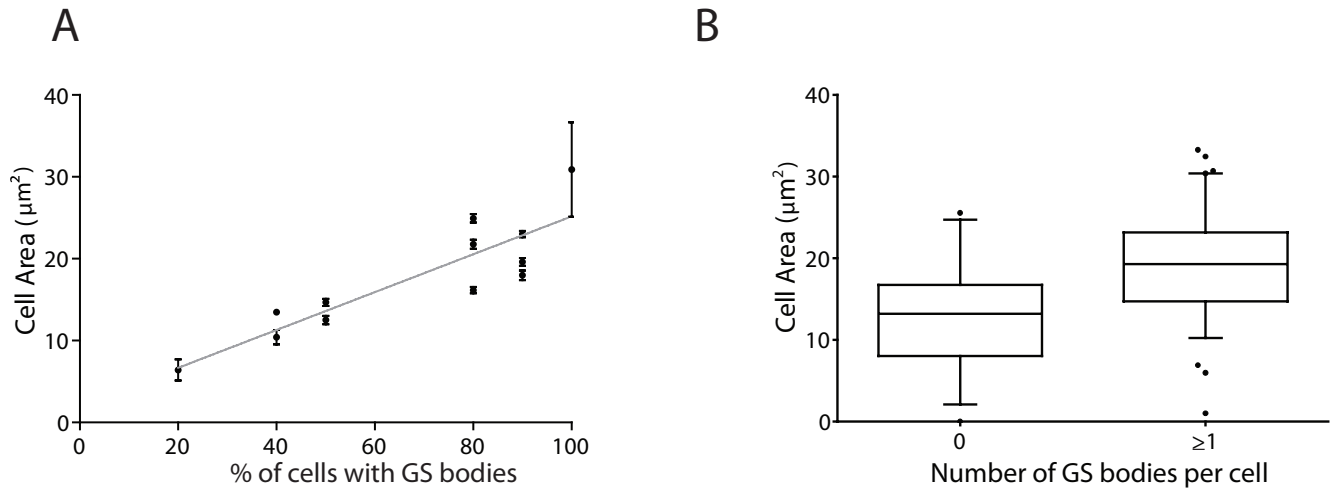
579 **Figure 2**

580
581

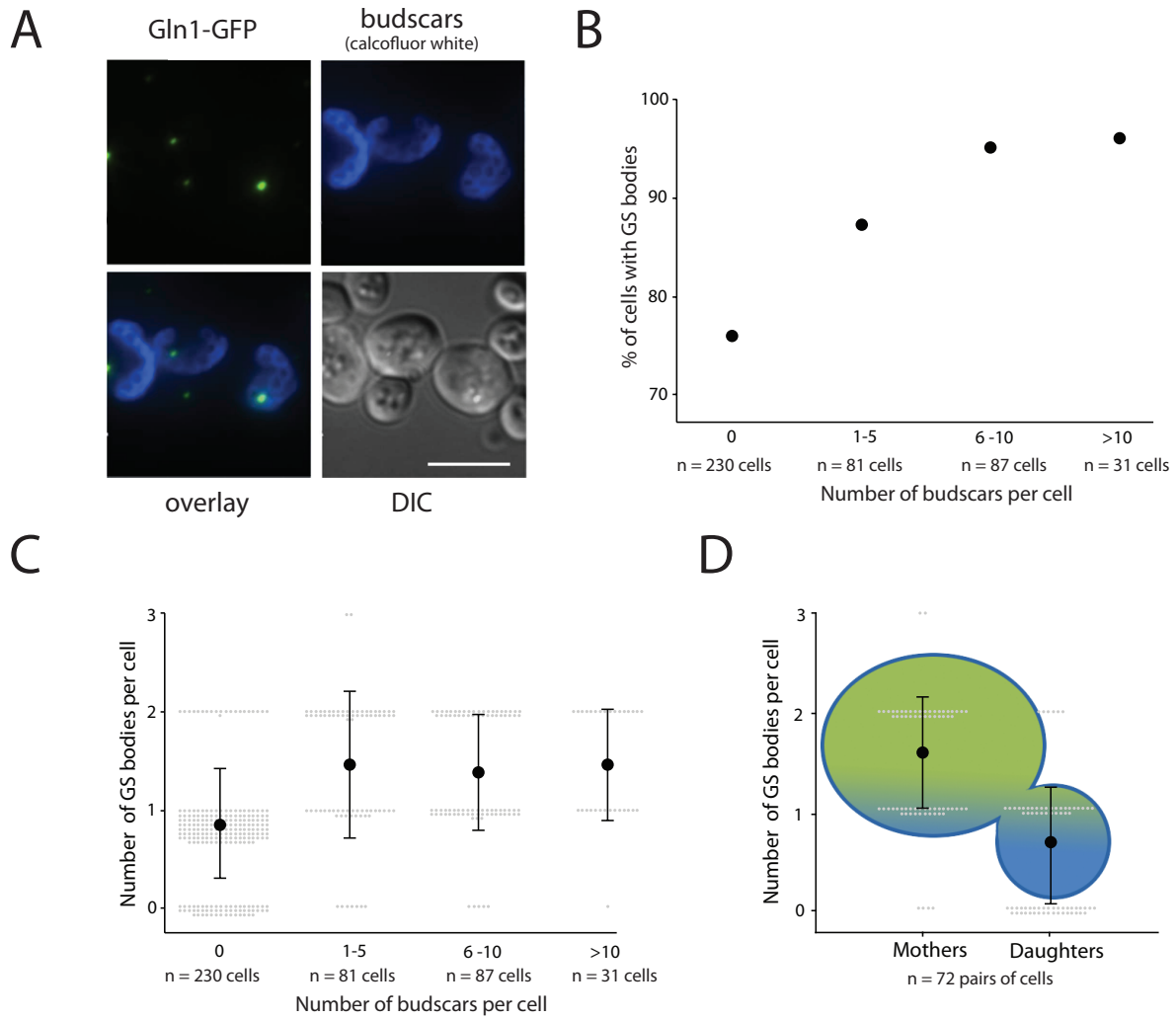


582
583
584
585
586
587
588
589
590
591
592
593
594
595
596
597
598
599
600
601
602
603
604
605
606
607

Figure 3.



609
610
611
612
613
614
615
616
617
618
619
620
621
622
623
624
625
626 **Figure 4.**
627
628
629
630
631
632
633
634
635
636
637
638
639
640



642
643
644
645
646
647
648
649
650
651
652
653
654
655
656

Figure 5.